1 Abstract

Forecasts of future ruptures are based on the brief historical record, paleoseismology, and geodetic strain accumulation. While we can never know the slip rate at every point on all faults in southern California, we can bound the *moment deficit rate* (MDR), or the integral of the slip deficit over each fault segment or fault system. In the past year we carefully tested a number of proposed methods for bounding the MDR using synthetic data and now we apply these methods to the faults system of Southern California and evaluate their performance. Preliminary results indicate that over the last 150 years, the accumulated seismic moment well exceeds that in the 1857 earthquake and is nearly that plus an additional M8 event.

2 Technical Report

Several studies have estimated coseismic moment or interseimic moment deficit rate using different methods. *Johnson et al.* (1994) was the first to bound the scalar moment during the 1992 Landers earthquake. *Murray and Segall* (2002) used Johnson's method combined with bootstrap resampling to estimate the interseismic moment deficit rate (MDR) at Parkfield prior to the 2004 earthquake, and showed that there is not a simple relationship between MDR and the recurrence time. *Maurer and Johnson* (2014) used both of these approaches to estimate the MDR on the creeping section of the San Andreas Fault (CSAF). *Johnson* (2013b) also estimated the MDR due to fully locked asperties on the CSAF. He adopted a model in which the fault is either creeping at constant resistive shear stress or locked. Many other studies that focus on slip deficit also cite a moment rate, but this is only a single value that comes from there best-fitting slip models (*Ryder and Burgmann*, 2008; *Jónsson et al.*, 2002; *Murray and Langbein*, 2006; *Murray et al.*, 2014; *Schmidt et al.*, 2005). However, these studies do not attempt to put rigorous bounds on the MDR.

In this study we present and evaluate methods for estimating bounds in the MDR itself. Our work is motivated by several important scientific and hazard questions, including the following: (1) Can we determine robust bounds on moment given the kinds of data available (GPS, InSAR, etc.)? (2) What current methods for estimating the MDR perform well in synthetic tests? (3) What is the current rate of moment deficit in Southern California, and how does it compare to the historic moment release. We show that the most straightforward methods based on Markov Chain Monte Carlo (MCMC) sampling fail to provide appropriate bounds on the MDR, the bootstrap provides optimistic coverage and fails in some cases, and an approach we term Constrained Optimization Bounding (COB) provides conservative, reliable bounds as long as data and prediction errors are known. Figure 1 compares the three methods discussed below for a simple, anti-plane strike-slip fault synthetic test.

2.1 Bootstrap

Bootstrapping is a well-known method for non-parametric parameter estimation (*Efron and Tibshirani*, 1994). To apply the bootstrap to estimate MDR, a random subsample of the data is selected with replacement and inverted to obtain slip. From slip, a bootstrap estimate of the MDR is computed (Equation 2.1). This is repeated many times to build a distribution, which can then be used to obtain confidence bounds by standard bootstrap techniques (*Efron and Tibshirani*, 1994). A simple approach is to use the empirical cdf from the bootstrap distribution.

The MDR is defined as

$$\dot{M}_d^{(b)} = \mu \sum_i a_i s_i^{(b)} \tag{2.1}$$

where μ is the shear modulus a_i is the area of the i-th fault element, and $s_i^{(b)}$ is the slip-deficit (or "backslip") in that element.

This approach has been applied at Parkfield (*Murray and Segall*, 2002) and the CSAF (*Maurer and Johnson*, 2014). Bootstrapping has the advantage that confidence bounds are clearly defined with no parametric assumptions about the errors in the data. It is also straightforward to implement and interpret.

The bootstrap can provide a reliable estimate of the moment rate when the problem is well-posed. *Murray and Segall* (2002) showed through synthetic tests that the bootstrap confidence intervals corresponded quite well with empirically derived confidence intervals. However, we have found through further testing that there are network/fault geometries for which the bootstrap fails badly (Figure 1a). This occurs when the network does not contain far-field stations that actually constrain the moment (or MDR). In this case we have found that the bootstrap intervals can be far too narrow. This appears to be the case for Southern California, presumably due to the high density of faults relative to the station spacing and fault locking depth, which means there is a paucity of stations sufficiently far from the faults to reliably estimate the MDR.

2.2 Constrained Optimization Bounding

This method was proposed by *Johnson et al.* (1994) to the coseismic moment of the Landers Earthquake. We solve the following system:

$$\begin{aligned} &\min_{\dot{\mathbf{s}}} \Phi = ||\mathbf{d} - \mathbf{G}\dot{\mathbf{s}}||_2^2 \\ &\text{s.t. } \dot{s}_{min} < \dot{s}_i < \dot{s}_{max} \quad \text{and} \quad \mu \sum_i a_i \dot{s}_i = \dot{M}_{test} \end{aligned} \tag{2.2}$$

where $\dot{s}_i$ is slip rate on the ith patch, with area a_i, and $\dot{M_{test}}$ is the MDR constraint. By systematically varying the constraint over the total space of possible moments (i.e., fully locked fault to fully creeping fault), we obtain a set of residual norms (or misfits) for each moment, which generally trace out a u-shaped curve as a function of $\dot{M_{test}}$. Due to the inequality constraints the residuals are not normally distributed, precluding the use of χ^2 statistics to determine confidence intervals.

Our approach is to modify the method outlined above in the following way: 1) Solve the

constrained optimization problem for each $\dot{M}_{test}$ as in Equation 2.2. The residuals are of the form

$$\Phi(\dot{M}_d = \dot{M}_{test}) = (\mathbf{d} - \mathbf{G}\dot{\mathbf{s}}_{test})^T \Sigma^{-1} (\mathbf{d} - \mathbf{G}\dot{\mathbf{s}}_{test}) = r_{M_{test}}^T \Sigma^{-1} r_{M_{test}}$$

the normalized residual norm for each moment. By analogy to Gaussian distributions, we transform the scaled residual norm to the distribution u:

$$u(\dot{M}_d) = Ce^{-\frac{1}{2}\Phi(\dot{M}_d)} \tag{2.3}$$

C is a normalizing constant to make u a density function that (we assume) approximates the likelihood on $\dot{M}_d, p(d|\dot{M}_d)$. Confidence bounds on MDR are found by using the empirical cumulative distribution function (CDF) of u. This approach is conservative, in the sense of at worst over predicting the bounds whether or not the stations are close or far from the fault (Figure 1).

2.3 Bayesian Methods

Although an obvious possibility, Bayesian approaches have not been previously used to estimate uncertainty in the MDR. We have extensively explored the use of Bayesian methods for building a probability distribution on MDR. The most obvious application of Bayesian methods with MCMC sampling assumes a uniform prior on slip in each element with bounds corresponding to either no slip or slip at the full long-term slip-rate. With no other regularization the slip is often assumed to be uncorrelated between elements. Consider the case with weak data constraint on the moment. The central limit theorem states that the sum of independent, random variables leads to a normal distribution, in this case with mean half-way between the bounds implied by the bounds on the slip-rate. This can be seen in the example shown in Figure 1. Future work may shed light on how to correctly apply Bayesian methods to estimate the distribution on MDR.

3 Application to Southern California

We use GPS velocities from the SCEC Community Motion Map 4 (Fig. 2a). We are investigating two distinct forward modeling schemes: 1) A simplified block model Fig. 2b), and 2) Full UCERF3 fault model, both in collaboration with Kaj Johnson. Much recent work has been done with elastic (and to a lesser degree, viscoelastic) block models, as well as the 'plate-block' model of *Johnson* (2013a). The advantage of such block models is that the slip-rates are kinematically consistent and described by a relatively few rotation poles.

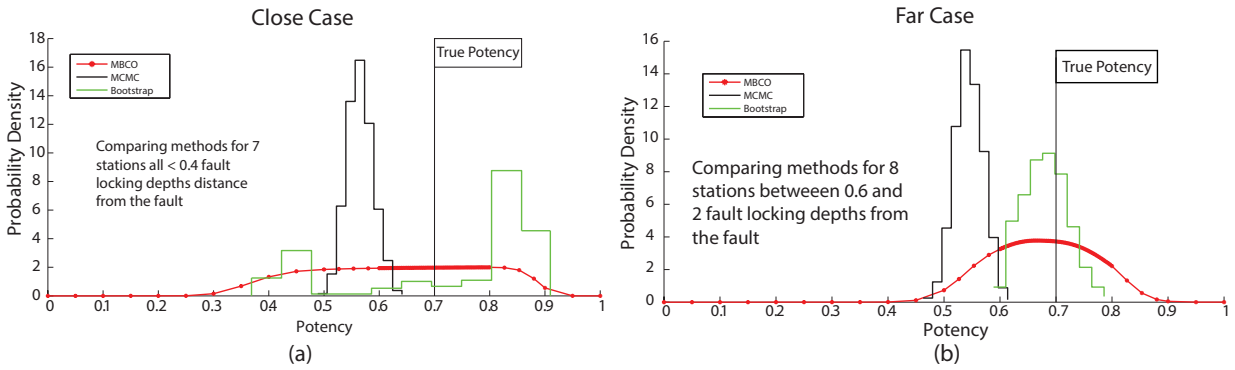

Figure 1: Synthetic test using an anti-plane, strike-slip geometry. Fault is discretized into N patches. The true MDR is shown by the vertical line. Comparison of three different moment bounding methods using an anti-plane synthetic case with several stations all located (a) close to the fault, and (b) far from the fault.

The disadvantage is that these models necessarily oversimplify the long-term kinematics of southern California, and either lump together or ignore smaller faults, especially in areas such as the Transverse Ranges and the Eastern California shear zone. It is difficult to know how much inaccuracies in the block models bias the estimated MDR. Results presented here are restricted to block models.

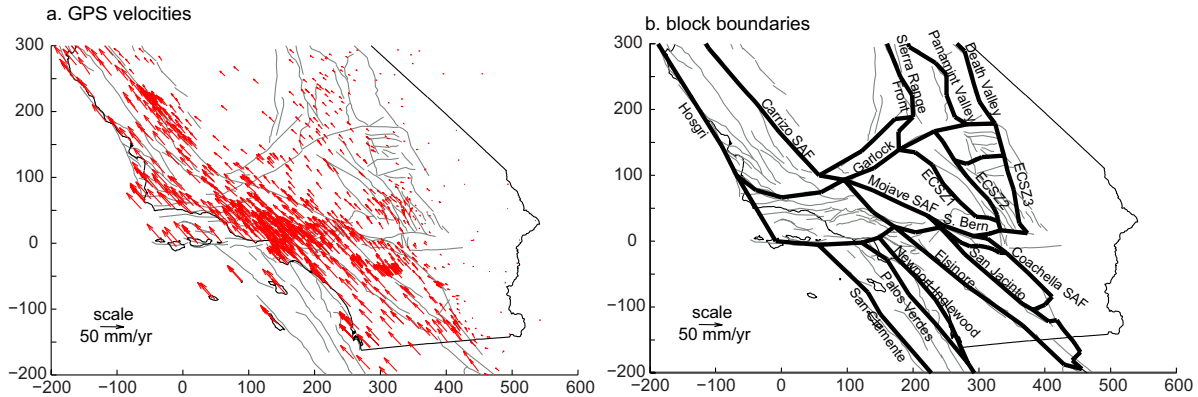

Figure 2: a) GPS velocities in southern California, b) generic block model. From *Johnson* (2013a)

We did not use the MCMC method for the reasons given in the description above, but we did run synthetic tests using the bootstrap and showed that the bootstrap fails to include the true moment and consistently underestimates the MDR. We believe that this results from the density of faults and the resultant lack of stations far from the faults which can constrain moment.

Figure 3 is a *coverage plot* based on synthetic data for the Southern California fault and station geometry using COB. The figure plots the number of times the true model is captured within a given confidence level (90%, 95%, etc.) versus the confidence level. In this case the

model captures the true value almost 100% of the time for a confidence level of only 60%, indicating that the method provides a conservative (pessimistic) estimate of the bounds on the MDR. A method that gave results below the theoretical one-to-one line would be to optimistic, or underestimate the width of the bounds.

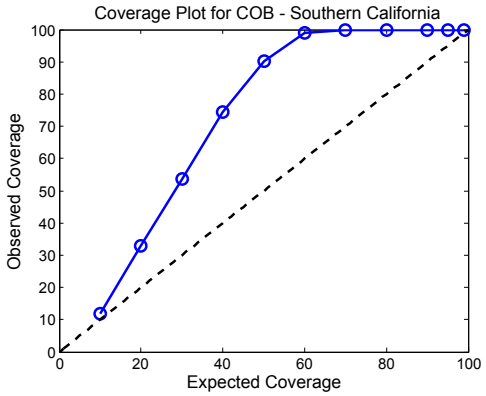

Figure 3: Coverage plot for the Southern California fault and station geometry using COB, indicates that our inferred bounds on the MDR are likely to be conservative.

To apply the COB approach to the SCEC Community Motion Map 4 velocities we must estimate the covariance matrix for the observations. We have tested two approaches. In the first, we assume tridiagonal covariance matrix, where the diagonal elements are the stated GPS velocity uncertainties scaled by the maximum likelihood estimate of a parameter σ^2 following *Fukuda and Johnson* (2008). The off-diagonal components are from empirically estimated correlations between the East and North components of the formal GPS uncertainties. This result is shown with the black curve in Figure 4. The second approach forms an empirical covariance matrix, computing the empirical spatial autocorrelation matrix of the residuals to the best-fitting model. In doing this we assume that the covariance is a function of distance between stations only. We demean the residuals and compute the sample variance and covariance for each distance bin and use this to construct the covariance matrix. This result is shown with the red curve in Figure 4. As expected the bounds are broader when we include correlations in the data between stations. The calculations assume that there is no slip deficit below a depth of 25 km.

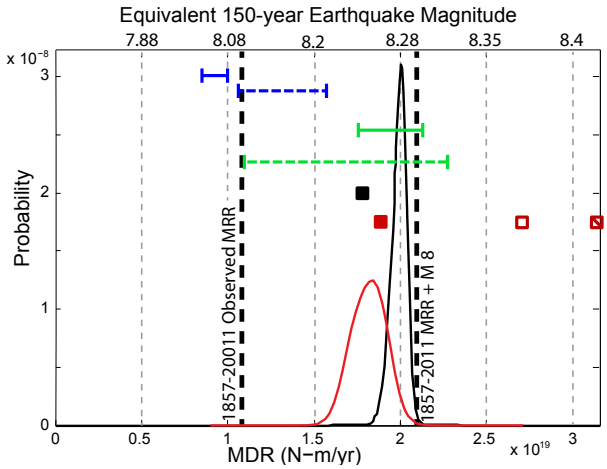

Figure 4: Constrained Optimization Bounding (COB) estimate of the total MDR for Southern California using a block model geometry. Black curve - pdf from COB assuming only East-North correlations in GPS data. Red curver - pdf from COB using empirically derived GPS covariance including interstation correlation (see text). Horizontal bars are estimates of the MDR from previous studies; the blue bars are Kostrov summation estimates; the solid line is *Ward* (1994) and *Savage and Simpson* (1997) and the dashed is *Ward* (1998). Green bars are from UCERF3; solid line is three different kinematic models and dashed line is an estimate using the geologic slip rates and assuming a fixed locking depth of 15 km everywhere. The black square is *Meade and Hager* (2005). Red squares are from *Johnson* (2013b); the solid square is a long-term-rigid elastic block model, J2 is an elastic plate-block model and equivalent to the block model results given by this study. The open square is a plate-block kinematic model and the crossed square is a viscoelastic cycle plate-block model. Vertical dashed black lines show the total moment released seismically since 1857 and total moment release plus an additional magnitude 8 event. The equivalent earthquake magnitudes shown assume all the moment deficit on all the faults is released at the same time.

4 Intellectual Merit and Broader Impacts

Our project accomplishes something new in that we place defensible bounds on the rate that seismic moment deficit rate accumulates. The moment deficit rate loosely measures the rate of strain energy accumulation and when integrated over the last 150 years, is presumed to bound the seismic moment that could occur in the near future. Strain based estimates of seismic hazard complement those based on paleoseismology.

In terms of broader impacts this project has contributed to the training of Ph.D. student Jeremy Maurer.

References

Efron, B., and R. J. Tibshirani (1994), *An Introduction to the Bootstrap*, CRC Press.

Fukuda, J., and K. M. Johnson (2008), A Fully Bayesian Inversion for Spatial Distribution of Fault Slip with Objective Smoothing, *Bulletin of the Seismological Society of America*, *98*(3), 1128–1146, doi:10.1785/0120070194.

Johnson, H. O., D. C. Agnew, and K. Hudnut (1994), Extremal bounds on earthquake movement from geodetic data: Application to the Landers earthquake, *Bulletin of the Seismological Society of America*, *84*(3), 660–667.

Johnson, K. (2013a), Slip rates and off-fault deformation in southern California inferred from GPS data and models, *Journal of Geophysical Research: Solid Earth*, *118*(10), 5643–5664.

Johnson, K. M. (2013b), Is stress accumulating on the creeping section of the San Andreas Fault?, *Geophysical Research Letters*, *40*(23), 6101–6105.

Jónsson, S., H. Zebker, P. Segall, and F. Amelung (2002), Fault slip distribution of the 1999 mw 7.1 hector mine, california, earthquake, estimated from satellite radar and gps measurements, *Bulletin of the Seismological Society of America*, *92*(4), 1377–1389, doi:10.1785/0120000922.

Maurer, J., and K. Johnson (2014), Fault coupling and potential for earthquakes on the creeping section of the central San Andreas Fault, *Journal of Geophysical Research: Solid Earth*, *119*(5), 4414–4428, doi:10.1002/2013JB010741.

Meade, B. J., and B. H. Hager (2005), Spatial localization of moment deficits in southern california, *Journal of Geophysical Research: Solid Earth*, *110*(B4), n/a–n/a, doi:10.1029/2004JB003331.

Minson, S. E., M. Simons, and J. L. Beck (2013), Bayesian inversion for finite fault earthquake source models I - theory and algorithm, *Geophysical Journal International*, doi:10.1093/gji/ggt180.

Murray, J., and J. Langbein (2006), Slip on the San Andreas Fault at Parkfield, California, over Two Earthquake Cycles, and the Implications for Seismic Hazard, *Bulletin of the Seismological Society of America*, *96*(4B), S283–S303, doi:10.1785/0120050820.

Murray, J., and P. Segall (2002), Testing time-predictable earthquake recurrence by direct measurement of strain accumulation and release, *Nature*, *419*, 287–291.

Murray, J. R., S. E. Minson, and J. L. Svarc (2014), Slip rates and spatially variable creep on faults of the northern San Andreas system inferred through Bayesian inversion of Global Positioning System data, *Journal of Geophysical Research: Solid Earth*, *119*(7), 6023–6047.

Ryder, I., and R. Burgmann (2008), Spatial variations in slip deficit on the central San Andreas Fault from InSAR, *Geophysical Journal International*, *175*(3), 837–852, doi:10.1111/j.1365-246X.2008.03938.x.

Savage, J., and R. Simpson (1997), Surface strain accumulation and the seismic moment tensor, *Bulletin of the Seismological Society of America*, *87*(5), 1345–1353.

Schmidt, D. A., R. Bürgmann, R. M. Nadeau, and M. dÁlessio (2005), Distribution of aseismic slip rate on the Hayward fault inferred from seismic and geodetic data, *J. Geophys. Res.*, *110*(B8), B08,406, doi:10.1029/2004JB003397.

Shen, Z.-K., R. W. King, D. C. Agnew, M. Wang, T. A. Herring, D. Dong, and P. Fang (2011), A unified analysis of crustal motion in southern california, 1970-2004: The scec crustal motion map, *Journal of Geophysical Research: Solid Earth*, *116*(B11), n/a–n/a, doi:10.1029/2011JB008549.

Ward, S. N. (1994), A multidisciplinary approach to seismic hazard in southern California, *Bulletin of the Seismological Society of America*, *84*(5), 1293–1309.

Ward, S. N. (1998), On the consistency of earthquake moment rates, geological fault data, and space geodetic strain: the United States, *Geophysical Journal International*, *134*(1), 172–186.